

Optimizing one dimensional superconducting diodes: Interplay of Rashba spin-orbit coupling and magnetic fields

Sayak Bhowmik,^{1,2,*} Dibyendu Samanta,^{3,*} Ashis K. Nandy,^{4,†} Arijit Saha,^{1,2,‡} and Sudeep Kumar Ghosh^{3,§}

¹*Institute of Physics, Sachivalaya Marg, Bhubaneswar, Orissa 751005, India*

²*Homi Bhabha National Institute, Training School Complex, Anushakti Nagar, Mumbai 400094, India*

³*Department of Physics, Indian Institute of Technology, Kanpur 208016, India*

⁴*School of Physical Sciences, National Institute of Science Education Research,*

An OCC of Homi Bhabha National Institute, Jatni 752050, India

(Dated: July 25, 2024)

The superconducting diode effect (SDE) refers to the non-reciprocal nature of the critical current (maximum current that a superconductor can withstand before turning into a normal metal) of a superconducting device. Here, we investigate SDE in helical superconductors with broken inversion and time-reversal symmetry, focusing on a prototypical Rashba nanowire device proximitized by an *s*-wave superconductor and subjected to external magnetic fields. Using a self-consistent Bogoliubov-de Gennes mean-field formalism, we analyze the interplay between linear and higher-order spin-orbit coupling (SOC), bulk supercurrents, and external magnetic fields. Our results demonstrate that Rashba nanowires with only linear SOC can achieve incredibly large diode efficiency $\gtrsim 45\%$ through the interplay of longitudinal and transverse magnetic fields. Notably, higher-order SOC enables finite diode efficiency even without a longitudinal Zeeman field, which can be utilized to reveal its presence and strength in nanowires. We present a comprehensive phase diagram of the device elucidating the emergent Fulde-Ferrell-Larkin-Ovchinnikov (FFLO) superconducting state and demonstrate that proximitized Rashba nanowires offer a versatile, practical platform for SDE, with potential realizations in existing material systems. These results provide crucial insights for optimizing SDE in nanoscale superconducting devices, paving the way for next-generation dissipationless quantum electronics.

I. INTRODUCTION

The invention of diodes marked a pivotal breakthrough in solid-state electronics, with their distinctive non-reciprocal current flow making them fundamental to semiconductor devices [1, 2]. In quantum materials, inversion and time-reversal symmetry crucially determine charge current nonreciprocity. Magnetochiral anisotropy (MCA), arising in systems with broken inversion symmetry [3], is a dominant mechanism for this effect. MCA leads to non-reciprocity in the magnetoresistance with respect to the current direction and can be greatly enhanced by superconducting correlations [4, 5]. In superconductors, MCA can lead to an extreme manifestation of nonreciprocity known as the superconducting diode effect (SDE), where resistance is zero in one current direction and non-zero in the other [6–8]. SDE thus realizes an ideal diode with perfect rectification. Such a scenario arises in the regime where the critical current that causes superconductor to normal metal transition differ in the opposite directions ($|J_c^+| \neq |J_c^-|$) [6, 7]. Recent experiments in engineered superlattice systems [8–10] and bulk materials/ thin films [5, 6, 11, 12] have spurred research interests into more efficient superconducting diode devices, including in twisted multilayer graphene [13, 14]

and transition metal dichalcogenides [15, 16].

The inversion symmetry breaking required for critical current non-reciprocity can be achieved through extrinsic mechanisms (e.g., asymmetric geometry or artificial superlattice potential [8, 10, 17]) or intrinsic mechanisms like Rashba spin-orbit coupling (SOC) [9, 18–25]. Correspondingly, SDE can be broadly classified into two types: extrinsic and intrinsic. Although predicted decades ago [26, 27], the mechanism of SDE is beginning to be understood only recently, leading to extensive investigations into its potential for dissipationless electronic circuits [6, 18, 19, 21, 28–32]. Recent theoretical studies [18, 19, 28, 29], using phenomenological Ginzburg-Landau theory and mean-field analysis of the two-dimensional Rashba-Zeeman Hubbard model, have shown that intrinsic SDE can arise in systems with broken inversion and time-reversal symmetry. In the helical superconducting ground state, this occurs due to asymmetry in Cooper pair momentum in the Fulde-Ferrell-Larkin-Ovchinnikov (FFLO) state [33, 34], resulting in Kramers non-degenerate *s*-wave Cooper pairs [6, 18, 28].

A Rashba nanowire device proximitized to an *s*-wave superconductor and subjected to external magnetic fields serves as a prototypical platform for realizing helical superconductivity [25, 31, 35–38]. While previous phenomenological/ non-self-consistent studies [25] demonstrated the potential for SDE in such systems, they reported low diode efficiencies ($\sim 2\%$). To enhance the relatively low diode efficiency of this device and better understand its properties, it's crucial to systematically investigate the superconducting order parameter

* These authors contributed equally to this work

† aknandy@niser.ac.in

‡ arijit@iopb.res.in

§ skghosh@iitk.ac.in

using self-consistent methods [19, 28, 31]. Recent studies [19, 28, 31] have shown that this approach can potentially uncover pathways for improvement across various parameters. In this paper, we address this gap through a comprehensive, self-consistent mean-field investigation of the interplay between various Rashba SOC terms and external magnetic fields in determining emergent FFLO pairing and highly efficient superconducting diodes in a Rashba nanowire device. We show that even with only linear Rashba SOC we can achieve a very large diode efficiency ($\gtrsim 45\%$) by suitably tuning the parameters in this system. We extend beyond linear Rashba SOC to include higher-order (cubic) Rashba SOC terms, which are not only naturally present in semiconducting nanowires [39–41] but also can dominate the normal state properties [42–49]. Notably, we demonstrate that higher-order Rashba SOC can induce finite diode efficiency ($\gtrsim 15\%$) even without longitudinal magnetic fields. This behavior differs qualitatively from the linear SOC case and can be used to detect the presence of higher-order SOC terms in the nanowire. Our study establishes the Rashba nanowire device as a promising platform for highly efficient superconducting diodes, crucial for advancing nanoscale superconducting electronics.

The remainder of this article is structured as follows. Sec. II introduces the proximity-induced Rashba nanowire device and outlines the self-consistent mean-field formalism used to investigate properties of the superconducting ground state in the nanowire. Sec. III presents our main findings on nonreciprocal charge transport in this device. We examine cases with both linear and higher-order Rashba SOC terms, exploring their interplay with Zeeman fields to optimize the SDE. Finally, Sec. IV summarizes our results, discusses potential material realizations, and proposes future research directions.

II. MODEL AND SELF-CONSISTENT MEAN-FIELD FORMALISM

We consider a single channel one-dimensional semiconducting nanowire along the z -direction with both linear and higher order Rashba SOC terms [39–41, 50] placed in close proximity to a three dimensional bulk s -wave superconductor as schematically shown in Fig. 1(a). In the presence of externally applied magnetic fields, the normal state physics of the nanowire is governed by the one-dimensional Rashba-Zeeman Hamiltonian [51]

$$\mathcal{H}_0 = \sum_{s,s'} \int dz \psi_s^\dagger(z) h_{ss'}(z) \psi_{s'}(z),$$

$$\hat{h}(z) = \frac{p_z^2}{2m} - \mu + \left(\frac{\alpha}{\hbar} p_z + \frac{\delta}{\hbar^3} p_z^3 \right) \sigma_x + \frac{\gamma}{\hbar^3} p_z^3 \sigma_y + \mathbf{B} \cdot \boldsymbol{\sigma}. \quad (1)$$

Here, the spin degree of freedom is labeled by $s, s' \in \{\uparrow, \downarrow\}$. $\psi_s^\dagger(z)$ creates a fermion at the position z with spin s , while $\boldsymbol{\sigma} = (\sigma_x, \sigma_y, \sigma_z)$ is the vector of the Pauli matrices in spin space and μ is the chemical potential. $p_z = \frac{\hbar}{i} \partial_z$

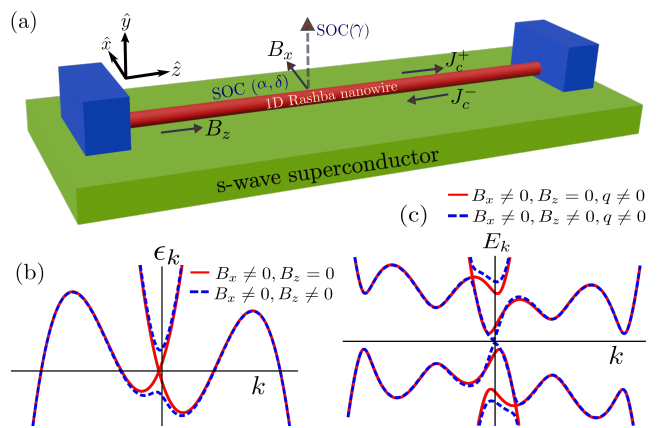


FIG. 1. **Schematic of the proximity-induced Rashba nanowire device:** (a) The schematic of our proposed device consisting of a Rashba nanowire in close proximity to an s -wave superconductor and in presence of external Zeeman fields: B_x and B_z to investigate SDE. The strength of the linear Rashba SOC is denoted by α , while the cubic Rashba SOC strengths are represented by δ and γ as illustrated in Eq. (2). (b) and (c): The dispersions of the normal state and the Bogoliubov quasi particles in the superconducting state are qualitatively shown in (b) and (c) respectively considering both linear and higher order SOC.

is the momentum operator in the direction of current flow (z -direction) within the nanowire. The strength of the usual linear Rashba SOC is denoted by α and the cubic Rashba SOC of strengths are δ and γ . The presence of Rashba SOC breaks the inversion symmetry of the system. The externally applied magnetic fields lead to the Zeeman term characterized by $\mathbf{B} = (B_x, B_y, B_z)$ that breaks time-reversal symmetry. We assume the radius of the nanowire to be small such that there is only one occupied mode, *i.e.*, single channel. This nanowire Hamiltonian [Eq. (1)] in momentum space can be written as

$$\mathcal{H}_0 = \sum_{s,s'} \sum_k c_{k,s}^\dagger h_{ss'}(k) c_{k,s'},$$

$$\hat{h}(k) = \xi_k + [(\alpha k + \delta k^3) \sigma_x + \gamma k^3 \sigma_y] + \mathbf{B} \cdot \boldsymbol{\sigma}. \quad (2)$$

Here, k represents the momentum along the nanowire (z -direction) and $\xi_k = \frac{\hbar^2 k^2}{2m} - \mu$. The bulk energy spectrum of the nanowire obtained by diagonalizing \hat{h}_k is given by

$$\epsilon_{\pm}(k) = \xi_k \pm \sqrt{(\alpha k + \delta k^3 + B_x)^2 + (\gamma k^3 + B_y)^2 + B_z^2}$$

where, \pm label the two helicity bands. Note that, the Zeeman field B_z (longitudinal field) opens a Zeeman gap while B_x (transverse field) creates asymmetry between the two bands as schematically shown in Fig. 1(b). On the other hand, B_y opens up a gap as well as creates band asymmetry (not shown). Throughout the majority of this paper, we will discuss the results with $B_y = 0$

for simplicity and will separately discuss the effects of nonzero B_y for completeness.

We seek to elucidate the nature of the superconducting ground state in the Rashba nanowire in the presence of s -wave superconducting correlations that can be induced via the proximity effect in presence of a bulk s -wave superconductor, as well as supercurrents (see Fig. 1(a)). In general, the presence of supercurrents can lead to a superconducting state with finite momentum Cooper pairs termed as the FFLO state. To establish that, we consider an attractive Hubbard type interaction in the bulk s -wave superconductor described by the Hamiltonian

$$\mathcal{H}_I = -\frac{U}{2} \sum_{s,s'} \int d^3\mathbf{r} \psi_s^\dagger(\mathbf{r}) \psi_{s'}^\dagger(\mathbf{r}) \psi_{s'}(\mathbf{r}) \psi_s(\mathbf{r}), \quad (3)$$

where, U is the attractive Hubbard interaction strength. We now decouple the Hubbard interaction term (\mathcal{H}_I) in the finite momentum s -wave channel within the mean-field approximation [23, 28, 31] and consider these correlations to be proximity induced in the nanowire. Then, using the Bogoliubov de-Gennes (BdG) mean-field formalism the effective Hamiltonian of the nanowire takes the form

$$\mathcal{H} = \frac{1}{2} \int dz \Psi^\dagger(z) \mathcal{H}_{BdG}(z) \Psi(z) + \mathcal{E}_0, \quad (4)$$

$$\mathcal{H}_{BdG}(z) = \begin{bmatrix} \hat{h}(z) & \hat{\Delta}(z) \\ -\hat{\Delta}^*(z) & -\hat{h}^*(z) \end{bmatrix}; \quad \hat{\Delta}(z) = -i\sigma_y \Delta e^{iqz},$$

where, $\Psi(z) = [\psi_\uparrow(z), \psi_\downarrow(z), \psi_\uparrow^\dagger(z), \psi_\downarrow^\dagger(z)]^T$ is the Nambu spinor inside the nanowire, $\mathcal{E}_0 = \frac{L}{V} |\Delta|^2$ with L denoting the length of the nanowire. The s -wave FFLO order parameter is given by $\Delta(z) = \Delta(-i\sigma_y) e^{iqz}$, where q is the Cooper pair momentum. The Hamiltonian in Eq. (4) effectively describes the physics of the Rashba nanowire device schematically shown in Fig. 1(a). To proceed further, we write the mean-field Hamiltonian [Eq. (4)] in the momentum space as

$$\mathcal{H} = \frac{1}{2} \sum_k \Psi_k^\dagger \mathcal{H}_{BdG}(k) \Psi_k + \mathcal{E}_0, \quad (5)$$

$$= \sum_{n,k} \left(E_{n,k} \gamma_{n,k}^\dagger \gamma_{n,k} - \frac{E_{n,k}}{2} \right) + \mathcal{E}_0,$$

with, $\mathcal{H}_{BdG}(k) = \begin{bmatrix} \hat{h}(k + \frac{q}{2}) & -i\sigma_y \Delta \\ i\sigma_y \Delta & -\hat{h}(-k + \frac{q}{2})^* \end{bmatrix}$.

Here, $\Psi_{\mathbf{k}} \equiv [c_{k+q/2,\uparrow}, c_{k+q/2,\downarrow}, c_{-k+q/2,\uparrow}^\dagger, c_{-k+q/2,\downarrow}^\dagger]^T$ and $E_{n,k}(q)$ denotes the Bogoliubov quasiparticle energies. The behavior of the Bogoliubov quasiparticle spectrum is schematically shown in Fig. 1(c). This depicts that the introduction of the pairing potential Δ opens a gap in the spectrum. As in the case of the nanowire spectrum, the asymmetry in BdG bands occurs due to the application of the Zeeman field B_x , and the Zeeman field B_z makes the bands distinctly gapped.

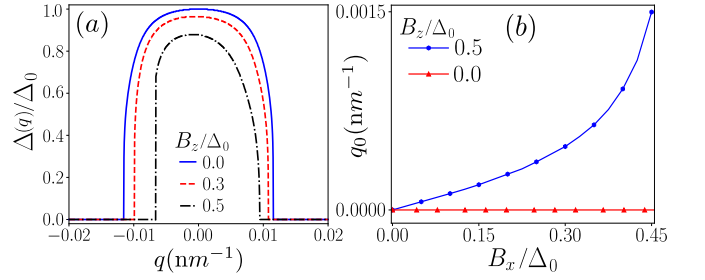


FIG. 2. **FFLO ground state with linear SOC:** (a) The self-consistent superconducting gap $\Delta(q)$ is shown as a function of the Cooper-pair momentum q (nm^{-1}) for $B_x/\Delta_0 = 0.3$ with only linear Rashba SOC ($\alpha = 100$ meV-nm). Δ_0 is the BCS gap in the absence of any external magnetic field ($\mathbf{B} = 0$). (b) The Cooper pair momentum of the FFLO ground state q_0 as a function of B_x . The presence of the FFLO ground state ($q_0 \neq 0$) is established only when both B_x and B_z are finite. Other model parameters are chosen as: $(B_y, \mu/\Delta_0, U, \beta^{-1}) = (0, 0.5, 25.55$ meV, 0.1 meV).

The condensation energy $\Omega(q)$ of the system, defined as the difference of free energy per unit length between the superconducting and normal state [28, 52], is

$$\Omega(q, \Delta) = F(q, \Delta) - F(q, 0), \quad (6)$$

where, $F(q, \Delta)$ is the free energy density of the nanowire given by

$$F(q, \Delta) = -\frac{1}{L\beta} \sum_{n,k} \ln \left[1 + e^{-\beta E_{n,k}(q)} \right] + \frac{|\Delta(q)|^2}{U}, \quad (7)$$

where, $\beta = (k_B T)^{-1}$ with k_B being the Boltzmann constant and T is the temperature.

We determine the order parameter $\Delta(q)$ for a given value of q by self-consistently solving the gap equation, obtained via minimizing the free energy $F(q, \Delta)$ in

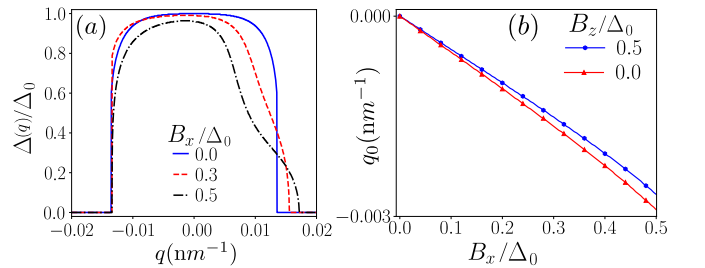


FIG. 3. **FFLO ground state with both linear and higher order SOC:** (a) The self-consistent superconducting gap $\Delta(q)$ is depicted as a function of Cooper-pair momentum q for $B_z = 0$ with both the linear Rashba SOC term ($\alpha = 100$ meV-nm) and the cubic Rashba SOC terms ($\delta = \gamma = 10$ eV-nm³). (b) The Cooper pair momentum of the FFLO ground state q_0 as a function of B_x is shown. Note that the FFLO state is stable even when $B_z = 0$ in the presence of a finite B_x . Other system parameters are chosen as: $(B_y, \mu/\Delta_0, U, \beta^{-1}) = (0, 0.5, 16.45$ meV, 0.1 meV).

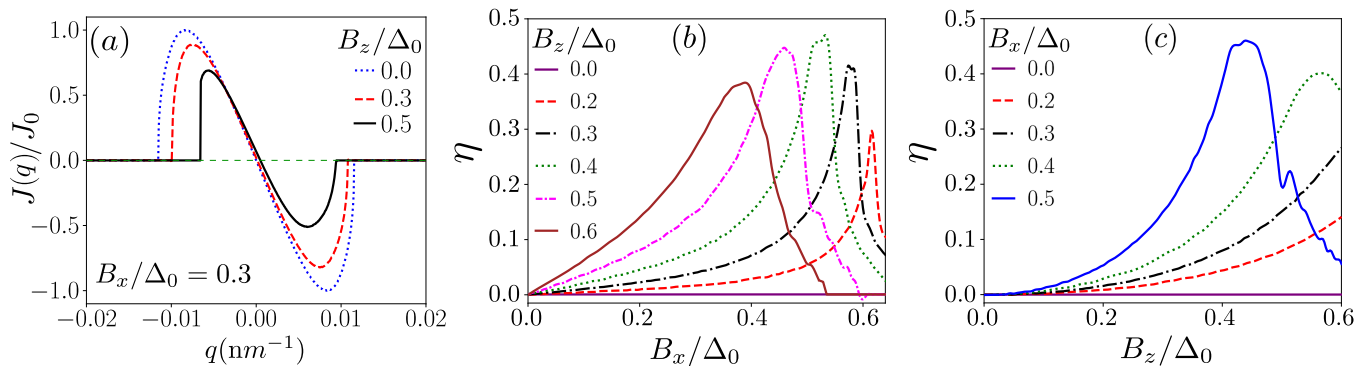


FIG. 4. **Superconducting diode effect with linear SOC:** (a) The supercurrent density (J) is shown as a function of q (nm^{-1}) considering solely linear Rashba SOC and $B_x/\Delta_0 = 0.3$. The nonreciprocity in the supercurrent, $J(q) \neq -J(-q)$, is achieved in this case only when both B_x and B_z are finite. It then leads to nonreciprocity in the critical supercurrents, $J_c^+ \neq |J_c^-|$, hence exhibiting a finite diode efficiency ($\eta \neq 0$). Here, $J_0 \equiv J_c(B_z = 0) = |J_c^+(B_z = 0)| = |J_c^-(B_z = 0)|$. (b) and (c): The corresponding diode efficiency (η) is shown as a function of B_x (with fixed B_z) and B_z (with fixed B_x) with only linear Rashba SOC in the panels (b) and (c) respectively. The system parameters are chosen as: $(B_y, \alpha, \mu/\Delta_0, U, \beta^{-1}) = (0, 100 \text{ meV-nm}, 0.5, 25.55 \text{ meV}, 0.1 \text{ meV})$.

Eq. (7), given by

$$\Delta(q) = -\frac{U}{L} \sum_{n,k} \frac{\partial E_{n,k}}{\partial \Delta^*} n_F(E_{n,k}) \quad (8)$$

where $n_F(E_{n,k}) = 1/(1 + e^{\beta E_{n,k}})$ is the Fermi function. Using the self-consistent solution of $\Delta(q)$ in Eq. (6), we optimize the condensation energy with respect to q to obtain the Cooper pair momentum (q_0) of the true FFLO superconducting ground state. The BCS gap in the absence of any external magnetic fields ($\mathbf{B} = 0$) is denoted by Δ_0 and we choose the value of U in such a way that we are in the weak coupling BCS regime with $\Delta_0 \sim 1 \text{ meV}$. In the rest of the paper, we present results in the low temperature limit choosing a fixed value of $\beta^{-1} = 0.1 \text{ meV}$ much smaller than Δ_0 .

The variation of the self-consistent solutions of the superconducting order parameter $\Delta(q)$ and the momentum of the Cooper pairs q_0 in the FFLO ground state with the external Zeeman fields are shown in Fig. 2 and Fig. 3 with only linear SOC case and, with both the linear and higher order SOC case respectively. We note from Fig 2(a) and Fig 3(a) that for both the cases the superconducting gap vanishes for a critical value of the Cooper pair momentum either above a positive value of $q = q_c^+$ or below a negative value of $q = q_c^-$. Fig 2(b) and Fig. 3(b) show that q_0 varies linearly with B_x for $B_x \ll \Delta_0$ for a given value of B_z . We note Fig 2(b) that in the case of only linear SOC q_0 is finite only when $B_z \neq 0$ and $B_x \neq 0$. This is because when only linear SOC is present the effect of the SOC can be gauged away by using a spin-dependent gauge transformation [53] and then when only $B_x \neq 0$ the band structure is symmetric leading to zero momentum Cooper pairs. However, when both $B_x, B_z \neq 0$, then in the transformed basis a spiral magnetic field texture is realized leading to momentum dependent asymmetry in the band structure and hence leading to finite momen-

tum Cooper pairs. In contrast, when both the linear and cubic SOC terms are present, the effect of SOC can not be gauged away and as a result only $B_x \neq 0$ is sufficient to give rise to $q_0 \neq 0$ in this case. Consequently, this feature also gets manifested in realizing finite SDE in this Rashba nanowire device, as extensively discussed in the next section.

III. NON-RECIPROCAL TRANSPORT

The supercurrent density $J(q)$ is computed from the condensation energy $\Omega(q, \Delta)$ in Eq. (6) as [18, 25, 28],

$$J(q) = -2e \frac{\partial \Omega(q, \Delta)}{\partial q}. \quad (9)$$

The sign of $J(q)$ indicates the direction of the supercurrent flow. The critical (optimal) values of the supercurrent along and opposite to the flow direction within the range $q_c^- \leq q \leq q_c^+$ for which the superconducting phase is stable, are denoted as J_c^+ and J_c^- respectively. When $|J_c^+| \neq |J_c^-|$, we have a finite SDE in the system and the efficiency or the quality factor of the SDE is defined as

$$\eta = \frac{|J_c^+| - |J_c^-|}{|J_c^+| + |J_c^-|}. \quad (10)$$

We first compute $J(q)$ over the range $q_c^- \leq q \leq q_c^+$ using the self-consistent solutions $\Delta(q)$ for each value of q (shown in Fig 2(a) and Fig 3(a) for example). Then finding its optimal values J_c^+ and J_c^- , we evaluate the diode efficiency (η) numerically. We systematically analyze the SDE in our Rashba nanowire device considering two broadly distinct scenarios: with only linear SOC and, with both linear and higher order SOC for various system parameters as discussed in the following two subsections.

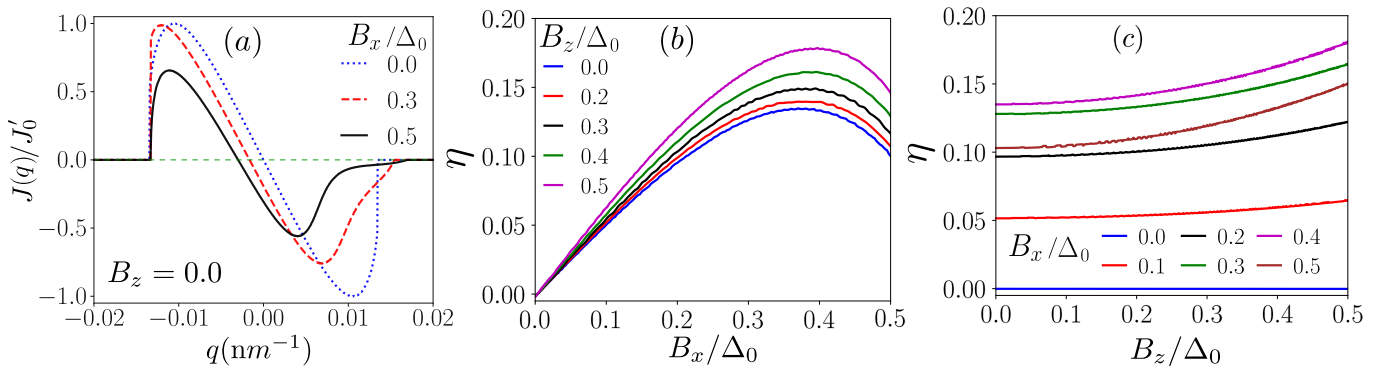


FIG. 5. **Superconducting diode effect with both linear and higher order SOC:** (a) The supercurrent density (J) as a function of q (nm^{-1}) with both cubic Rashba SOC ($\delta = \gamma = 10 \text{ eV}\cdot\text{nm}^3$) and linear Rashba SOC ($\alpha = 100 \text{ meV}\cdot\text{nm}$) choosing $B_z = 0$. The nonreciprocity in the critical supercurrents: $|J_c^+| \neq |J_c^-|$ (also implying a finite diode efficiency $\eta \neq 0$) is achieved for any finite value of B_x . Here, $J'_0 \equiv J_c(B_x = B_z = 0) = |J_c^+(B_x = B_z = 0)| = |J_c^-(B_x = B_z = 0)|$. (b) and (c): The corresponding diode efficiency (η) is depicted as a function of B_x (with fixed B_z) and B_z (with fixed B_x) in the panels (b) and (c) respectively. We have chosen the other model parameters as: $(B_y, \mu/\Delta_0, U, \beta^{-1}) = (0, 0.5, 16.45 \text{ meV}, 0.1 \text{ meV})$.

A. Case-I: Rashba nanowire with only linear SOC

In the presence of only linear Rashba SOC, we uncover the SDE by investigating the behavior of the supercurrent density ($J(q)$) and the diode efficiency (η) for different system parameters as presented in Fig. 4. Fig. 4(a) shows that the supercurrent density is symmetric with respect to q for $B_z = 0$ even with $B_x \neq 0$ [25]. We note that as we start increasing the magnitude of B_z with $B_x \neq 0$, $J(q)$ becomes more and more asymmetric, leading to nonreciprocal critical supercurrents, $|J_c^+| \neq |J_c^-|$ and hence to finite SDE. This is a direct consequence of the fact that the presence of FFLO state and the asymmetry in critical momenta: $|q_c^+| \neq |q_c^-|$ is distinctly realized only in presence of both the fields B_x, B_z as noted in Fig. 2(a).

The diode efficiency as a function of B_x for fixed values of B_z and as a function of B_z for fixed values of B_x are shown in Fig. 4(b) and Fig. 4(c) respectively. In both cases, η increases linearly at low field strengths, reaches a maximum at moderate values, and then decreases to zero as the field strengths continue to intensify. This behavior can be understood as a consequence of a competition between the asymmetry in the band structure of the system and changes in the superconducting pairing susceptibility as the magnetic field strengths are varied, consistent with previous studies [18, 20]. Note that, the self-consistent BCS gap vanishes for very large values of the Zeeman fields B_x and B_z consequently leading to zero efficiency, however the resultant nanowire spectrum might still be gapped like an ordinary insulator.

Preceding investigations on a Rashba nanowire featuring only linear Rashba SOC [25] reported maximum diode efficiency of $\sim 2\%$, where the superconducting order parameter has been fixed to a particular value. Contrastingly, our study reveals that the self-consistently derived superconducting order parameter within the full parameters space has significant influence on the perfor-

mance of the diode where the highest η value is found to be $\gtrsim 45\%$. This is evident from calculation presented in Fig. 4(b,c). The vanishing of the superconducting gap within our self-consistent treatment necessitates restricting the maximum values of the magnetic fields used in our model. We note that in this case B_y also plays a similar role as B_z due to the geometry of the setup (see Fig. 1(a)) under consideration and hence further analysis considering $B_y \neq 0$ is not presented. However, B_y plays a significant and distinct role when we consider the effect of cubic Rashba SOC terms as discussed in the next subsection.

B. Case-II: Rashba nanowire with both linear and higher order SOC

The variation of $J(q)$ and η in the case when both the linear ($\alpha \neq 0$) and cubic Rashba SOC terms ($\delta, \gamma \neq 0$) are present in the nanowire are shown in Fig. 5. First of all, comparing Fig. 5(a) with Fig. 4(a), we note that the cubic Rashba SOC terms interestingly lead to asymmetry in $J(q)$ even with $B_z = 0$ as long as $B_x \neq 0$. This leads to nonreciprocal critical supercurrents, $|J_c^+| \neq |J_c^-|$ with a single magnetic field $B_x \neq 0$ in contrast to only linear SOC case discussed earlier. The variation of η with the magnetic fields B_x and B_z with $B_y = 0$ are shown in Fig. 5(b, c). We note from Fig. 5(b) that the diode efficiency at a fixed B_z exhibits a linear increase as a function of B_x for small values of $B_x \ll \Delta_0$, eventually attaining a maxima around $B_x/\Delta_0 = 0.4$ similar to the case with only linear Rashba SOC described earlier. This behavior, as in the earlier linear SOC case [18, 20], results from two competing effects: the system's asymmetric band structure versus changes in superconducting pairing susceptibility as magnetic field strength varies. The maximum efficiency increases as one increases the magnitude of B_z . However, η shows only marginal en-

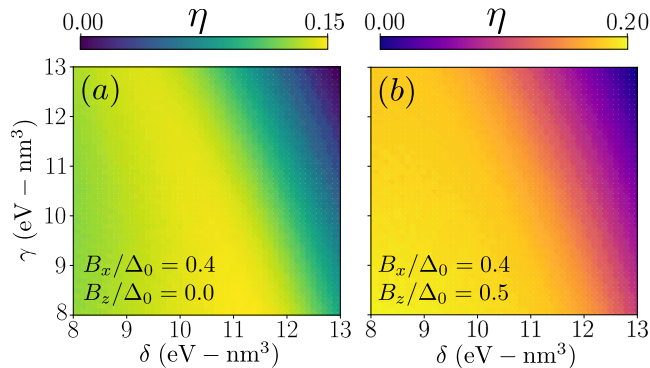


FIG. 6. **Diode efficiency phase diagram with both linear and higher order SOC:** The variation of the diode efficiency η is shown in the plane of cubic Rashba SOC parameters $\delta - \gamma$ choosing “optimal” values of the Zeeman fields $(B_x/\Delta_0, B_z/\Delta_0) = (0.4, 0.0)$ in panel (a) and $(B_x/\Delta_0, B_z/\Delta_0) = (0.4, 0.5)$ in panel (b), respectively. We note a small enhancement in the maximum value of η for finite B_z . The other system parameters are chosen as: $(B_y, \alpha, \mu/\Delta_0, \beta^{-1}) = (0, 100 \text{ meV-nm}, 0.5, 0.1 \text{ meV})$.

hancement at a fixed value of B_x when B_z is varied as depicted in Fig. 5(c).

Modifying the values of δ and γ evidently changes the band dispersions in the normal and superconducting state of the system and consequently the efficiency of the superconducting diode will also change. We depict the diode efficiency phase diagrams in the $\delta - \gamma$ plane in Fig. 6. We obtain the phase diagrams by varying U for every configuration of (δ, γ) such that the self-consistent BCS gap Δ_0 remains fixed. For the $B_z = 0$ and $B_x \neq 0$ case, we can achieve a peak diode efficiency of approximately 15% for an optimal choice of higher-order Rashba SOC parameters as shown in Fig. 6(a). We emphasize that this behavior is qualitatively different from the linear SOC case, where the efficiency is zero with only the B_x field. This distinctive response, arising solely from higher-order SOC terms, provides a method to detect and quantify the strength of these terms in a nanowire device.

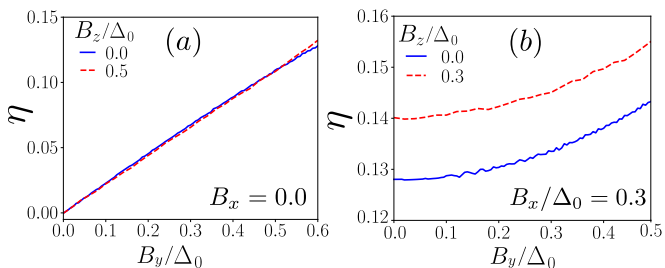


FIG. 7. The diode efficiency η as a function of B_y with both linear and cubic Rashba SOC terms for $B_x = 0$ and finite $B_x/\Delta_0 = 0.3$ are shown in (a) and (b) respectively. The chosen model parameters are $(\alpha, \delta, \gamma, \mu/\Delta_0, \beta^{-1}) = (100 \text{ meV-nm}, 10 \text{ eV-nm}^3, 10 \text{ eV-nm}^3, 0.5, 0.1 \text{ meV})$.

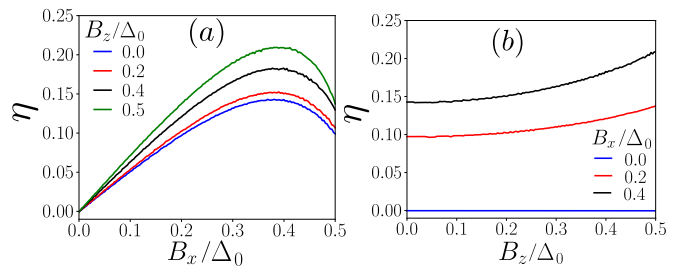


FIG. 8. The diode efficiency (η) with linear SOC and with cubic SOC of different type where $\delta = 10 \text{ eV-nm}^3$ but $\gamma = 0$ as a function of B_x (with fixed B_z) and B_z (with fixed B_x) are shown in (a) and (b) respectively. Other parameters are: $(\alpha, \mu/\Delta_0, B_y, \beta^{-1}) = (100 \text{ meV-nm}, 0.5, 0, 0.1 \text{ meV})$.

The application of an additional magnetic field B_z readily elevates η to approximately 20%, as illustrated in Fig. 6(b) since effects of both the linear and cubic SOC terms are relevant. Note that the presence of highly asymmetric behavior in the supercurrent, given a specific set of system parameters, does not necessarily guarantee a corresponding high level of non-reciprocity in the supercurrents. As is evident from Fig. 6(a,b), the system might exhibit nearly negligible diode effect ($\eta \sim 0$) even though the parameters are set such that there is asymmetry in supercurrent (top right corners of Fig. 6(a,b)).

Note that the results discussed so far were obtained by fixing $B_y = 0$. The effect of finite B_y in η is shown in the Fig. 7. In this case, B_y serves the role of both B_x and B_z in realizing a finite SDE by creating both gap and asymmetry in the band structure. Fig. 7(a) and Fig. 7(b) show that the application of B_y produces systematic increase in η with increasing B_y for different values of B_z with $B_x = 0$ and $B_x \neq 0$ respectively. However, B_y can not increase the efficiency beyond a certain limit because the superconducting state becomes unstable after some value of B_y when the other magnetic fields are present as well.

For completeness, we consider a special case with a different type of the higher order Rashba SOC terms [50] when only $\delta \neq 0$ and $\gamma = 0$ (with $\alpha \neq 0$ as usual). The variation of the corresponding diode efficiencies with the magnetic fields are shown in Fig. 8. A finite diode efficiency with a maximum of $\sim 12\%$ even in presence of a finite B_x only is obtained as shown in Fig. 8(a) which is also in contrast to the linear SOC case. Thus the presence of even a single cubic Rashba parameter δ is sufficient to manifest SDE. By further application of B_z the diode efficiency η is readily enhanced upto $\sim 21\%$ as a function of B_x shown in Fig. 8(a). There is only a marginal increase in efficiency by increasing B_z for fixed B_x as shown in the Fig. 8(b).

IV. SUMMARY AND CONCLUSIONS

This article analyzes how the interplay between linear and cubic Rashba SOC terms, combined with external Zeeman fields, can optimize the efficiency of SDE in a proximitized one-dimensional nanowire device. Using self-consistent mean-field analysis, we demonstrate that SDE, characterized by nonreciprocal critical currents ($|J_c^+| \neq |J_c^-|$), arises from Cooper pair momentum asymmetry in the helical superconducting ground state of this time-reversal and inversion symmetry broken system. Remarkably, we achieve a diode efficiency $\eta \gtrsim 45\%$ with only linear Rashba SOC significantly higher than the previously reported efficiency of $\eta \sim 2\%$ from non-self-consistent analyses [25]. In this case with only linear SOC, at least two magnetic fields are required to obtain a finite diode efficiency: one along the SOC direction and one perpendicular to it. This requirement stems from the fact that linear SOC effects can be eliminated through a spin-dependent gauge transformation [53], resulting in a conventional BCS superconducting state with zero Cooper pair momentum when only one Zeeman field is present. However, the presence of two orthogonal Zeeman fields creates a spiral magnetic field texture via the gauge transformation, leading to momentum-dependent band asymmetry and asymmetric FFLO Cooper pairs [53]. In contrast, higher-order SOC effects cannot be eliminated via gauge transformations, allowing for finite diode efficiency even with only one Zeeman field unlike the linear SOC case and this behavior can be used to detect the presence of higher-order SOC in nanowires. However, including higher-order SOC doesn't improve the maximum diode efficiency (only $\eta \sim 20\%$), this value remains significant compared to previously reported diode efficiencies [6, 25]. Our results underscore the importance of self-consistently determining the order parameter of the superconducting ground state to fully

understand the capability and optimize Rashba nanowire devices as superconducting diodes.

Our findings can be readily experimentally tested in spin orbit coupled Rashba nanowires [51, 54–56] such as zinc-blende InSb and wurtzite InAs, with lengths of approximately 100 nm, where cubic Rashba SOC interactions are significant depending on the growth direction [39]. Superconductivity can be proximity induced in these nanowires by common bulk *s*-wave superconductors like Nb or Al. Future research directions include investigating SDE in proximity-induced multichannel Rashba nanowires with overlapping channels [51, 57–59], extending beyond the single-channel case examined here. Additionally, the influence of topological superconductivity realized in the nanowire and the nanowire device geometry on SDE warrants further exploration [60–65]. An intriguing prospect is the potential replication of magnetic field effects using electric fields via the Rashba-Edelstein effect [6, 66–68], which could lead to the realization of field-free SDE.

V. ACKNOWLEDGMENTS

SKG acknowledges financial support from SERB, Government of India via the Startup Research Grant: SRG/2023/000934 and IIT Kanpur via the Initiation Grant (IITK/PHY/2022116). A.K.N. acknowledges the financial support from Department of Atomic Energy (DAE), Govt. of India, through the project Basic Research in Physical and Multidisciplinary Sciences via RIN4001. The authors acknowledge discussions with Koushik Mandal, Krishnendu Sengupta and Amit Agarwal. DS and SKG utilized the *Andromeda* server at IIT Kanpur for numerical calculations. SB and AS acknowledge SAMKHYA: High-Performance Computing Facility provided by Institute of Physics, Bhubaneswar, for numerical computations.

-
- [1] J. H. Scaff and R. S. Ohl, “Development of silicon crystal rectifiers for microwave radar receivers,” *The Bell System Technical Journal* **26**, 1–30 (1947).
 - [2] W. Shockley, “The theory of p-n junctions in semiconductors and p-n junction transistors,” *The Bell System Technical Journal* **28**, 435–489 (1949).
 - [3] Yoshinori Tokura and Naoto Nagaosa, “Nonreciprocal responses from non-centrosymmetric quantum materials,” *Nature communications* **9**, 3740 (2018).
 - [4] F Qin, W Shi, T Ideue, M Yoshida, A Zak, Reshef Tenne, T Kikitsu, D Inoue, D Hashizume, and Y Iwasa, “Superconductivity in a chiral nanotube,” *Nature communications* **8**, 14465 (2017).
 - [5] Ryohei Wakatsuki, Yu Saito, Shintaro Hoshino, Yuki M Itahashi, Toshiya Ideue, Motohiko Ezawa, Yoshihiro Iwasa, and Naoto Nagaosa, “Nonreciprocal charge transport in noncentrosymmetric superconductors,” *Science advances* **3**, e1602390 (2017).
 - [6] Muhammad Nadeem, Michael S Fuhrer, and Xiaolin Wang, “The superconducting diode effect,” *Nature Reviews Physics* **5**, 558–577 (2023).
 - [7] Naoto Nagaosa and Yoichi Yanase, “Nonreciprocal transport and optical phenomena in quantum materials,” *Annual Review of Condensed Matter Physics* **15**, 63–83 (2024).
 - [8] Hideki Narita and Teruo Ono, “Superconducting diode effect in artificial superlattices,” *JSAP Review* **2024**, 240206 (2024).
 - [9] Fuyuki Ando, Yuta Miyasaka, Tian Li, Jun Ishizuka, Tomonori Arakawa, Yoichi Shiota, Takahiro Moriyama, Yoichi Yanase, and Teruo Ono, “Observation of superconducting diode effect,” *Nature* **584**, 373–376 (2020).
 - [10] Ananthesh Sundaresh, Jukka I Väyrynen, Yuli Lyanda-Geller, and Leonid P Rokhinson, “Diamagnetic mechanism of critical current non-reciprocity in multilayered superconductors,” *Nature Communications* **14**, 1628 (2023).

- [11] Yuki M Itahashi, Toshiya Ideue, Yu Saito, Sunao Shimizu, Takumi Ouchi, Tsutomu Nojima, and Yoshihiro Iwasa, “Nonreciprocal transport in gate-induced polar superconductor SrTiO₃,” *Science advances* **6**, eaay9120 (2020).
- [12] Timo Schumann, Luca Galletti, Hanbyeol Jeong, Kaveh Ahadi, William M. Strickland, Salva Salmani-Rezaie, and Susanne Stemmer, “Possible signatures of mixed-parity superconductivity in doped polar SrTiO₃ films,” *Phys. Rev. B* **101**, 100503 (2020).
- [13] Jiang-Xiazi Lin, Phum Siriviboon, Harley D Scammell, Song Liu, Daniel Rhodes, K Watanabe, T Taniguchi, James Hone, Mathias S Scheurer, and JIA Li, “Zero-field superconducting diode effect in small-twist-angle trilayer graphene,” *Nature Physics* **18**, 1221–1227 (2022).
- [14] J Díez-Mérida, A Díez-Carlón, SY Yang, Y-M Xie, X-J Gao, J Senior, K Watanabe, T Taniguchi, X Lu, Andrew P Higginbotham, *et al.*, “Symmetry-broken josephson junctions and superconducting diodes in magic-angle twisted bilayer graphene,” *Nature Communications* **14**, 2396 (2023).
- [15] Lorenz Bauriedl, Christian Bäuml, Lorenz Fuchs, Christian Baumgartner, Nicolas Paulik, Jonas M Bauer, Kai-Qiang Lin, John M Lupton, Takashi Taniguchi, Kenji Watanabe, *et al.*, “Supercurrent diode effect and magnetochiral anisotropy in few-layer NbSe₂,” *Nature communications* **13**, 4266 (2022).
- [16] Jonginn Yun, Suhan Son, Jeacheol Shin, Giung Park, Kaixuan Zhang, Young Jae Shin, Je-Geun Park, and Dohun Kim, “Magnetic proximity-induced superconducting diode effect and infinite magnetoresistance in a van der Waals heterostructure,” *Phys. Rev. Res.* **5**, L022064 (2023).
- [17] AA Burlakov, VL Gurtovoi, AI Il’in, Alexey V Nikulov, and VA Tulin, “Superconducting quantum interference device without josephson junctions,” *JETP letters* **99**, 169–173 (2014).
- [18] Noah F. Q. Yuan and Liang Fu, “Supercurrent diode effect and finite-momentum superconductors,” *Proceedings of the National Academy of Sciences* **119**, e2119548119 (2022).
- [19] S. Ilić and F. S. Bergeret, “Theory of the supercurrent diode effect in rashba superconductors with arbitrary disorder,” *Phys. Rev. Lett.* **128**, 177001 (2022).
- [20] Bianca Turini, Sedighe Salimian, Matteo Carrega, Andrea Iorio, Elia Strambini, Francesco Giazotto, Valentina Zannier, Lucia Sorba, and Stefan Heun, “Josephson diode effect in high-mobility insb nanoflags,” *Nano Letters* **22**, 8502–8508 (2022).
- [21] Mercè Roig, Panagiotis Kotetes, and Brian M. Andersen, “Superconducting diodes from magnetization gradients,” *Phys. Rev. B* **109**, 144503 (2024).
- [22] Klaus Halterman, Mohammad Alidoust, Ross Smith, and Spencer Starr, “Supercurrent diode effect, spin torques, and robust zero-energy peak in planar half-metallic trilayers,” *Phys. Rev. B* **105**, 104508 (2022).
- [23] Akito Daido and Youichi Yanase, “Superconducting diode effect and nonreciprocal transition lines,” *Phys. Rev. B* **106**, 205206 (2022).
- [24] T. Karabassov, I. V. Bobkova, A. A. Golubov, and A. S. Vasenko, “Hybrid helical state and superconducting diode effect in superconductor/ferromagnet/topological insulator heterostructures,” *Phys. Rev. B* **106**, 224509 (2022).
- [25] Henry F. Legg, Daniel Loss, and Jelena Klinovaja, “Superconducting diode effect due to magnetochiral anisotropy in topological insulators and Rashba nanowires,” *Phys. Rev. B* **106**, 104501 (2022).
- [26] LS Levitov, Yu V Nazarov, and GM Eliashberg, “Magnetostatics of superconductors without an inversion center,” *JETP Lett* **41**, 365 (1985).
- [27] Victor M Edelstein, “The ginzburg-landau equation for superconductors of polar symmetry,” *Journal of Physics: Condensed Matter* **8**, 339 (1996).
- [28] Akito Daido, Yuhei Ikeda, and Youichi Yanase, “Intrinsic superconducting diode effect,” *Phys. Rev. Lett.* **128**, 037001 (2022).
- [29] James Jun He, Yukio Tanaka, and Naoto Nagaosa, “A phenomenological theory of superconductor diodes,” *New Journal of Physics* **24**, 053014 (2022).
- [30] Banabir Pal, Anirban Chakraborty, Pranava K Sivakumar, Margarita Davydova, Ajesh K Gopi, Avanindra K Pandeya, Jonas A Krieger, Yang Zhang, Mihir Date, Sailong Ju, *et al.*, “Josephson diode effect from cooper pair momentum in a topological semimetal,” *Nature physics* **18**, 1228–1233 (2022).
- [31] Tatiana de Picoli, Zane Blood, Yuli Lyanda-Geller, and Jukka I. Väyrynen, “Superconducting diode effect in quasi-one-dimensional systems,” *Phys. Rev. B* **107**, 224518 (2023).
- [32] Sayan Banerjee and Mathias S. Scheurer, “Enhanced superconducting diode effect due to coexisting phases,” *Phys. Rev. Lett.* **132**, 046003 (2024).
- [33] Peter Fulde and Richard A. Ferrell, “Superconductivity in a strong spin-exchange field,” *Phys. Rev.* **135**, A550–A563 (1964).
- [34] AI Larkin and Yu N Ovchinnikov, “Nonuniform state of superconductors,” *Soviet Physics-JETP* **20**, 762–762 (1965).
- [35] Yuval Oreg, Gil Refael, and Felix von Oppen, “Helical liquids and majorana bound states in quantum wires,” *Phys. Rev. Lett.* **105**, 177002 (2010).
- [36] Jay D. Sau, Sumanta Tewari, Roman M. Lutchyn, Tudor D. Stanescu, and S. Das Sarma, “Non-abelian quantum order in spin-orbit-coupled semiconductors: Search for topological majorana particles in solid-state systems,” *Phys. Rev. B* **82**, 214509 (2010).
- [37] Roman M. Lutchyn, Jay D. Sau, and S. Das Sarma, “Majorana fermions and a topological phase transition in semiconductor-superconductor heterostructures,” *Phys. Rev. Lett.* **105**, 077001 (2010).
- [38] Tudor D. Stanescu, Roman M. Lutchyn, and S. Das Sarma, “Majorana fermions in semiconductor nanowires,” *Phys. Rev. B* **84**, 144522 (2011).
- [39] Tiago Campos, Paulo E. Faria Junior, Martin Gmitra, Guilherme M. Sipahi, and Jaroslav Fabian, “Spin-orbit coupling effects in zinc-blende insb and wurtzite insb nanowires: Realistic calculations with multiband $\mathbf{k} \cdot \mathbf{p}$ method,” *Phys. Rev. B* **97**, 245402 (2018).
- [40] Michael Kammermeier, Paul Wenk, Florian Dirnberger, Dominique Bougeard, and John Schliemann, “Spin relaxation in wurtzite nanowires,” *Phys. Rev. B* **98**, 035407 (2018).
- [41] Junpei Sonehara, Michael Kammermeier, Dai Sato, Daisuke Iizasa, Ulrich Zülicke, Shutaro Karube, Junsaku Nitta, and Makoto Kohda, “Anisotropic spin dynamics in semiconductor narrow wires from the interplay between spin-orbit interaction and planar magnetic field,”

- Phys. Rev. B* **105**, 094434 (2022).
- [42] Sz. Vajna, E. Simon, A. Szilva, K. Palotas, B. Ujfalussy, and L. Szunyogh, “Higher-order contributions to the Rashba-Bychkov effect with application to the Bi/Ag(111) surface alloy,” *Phys. Rev. B* **85**, 075404 (2012).
- [43] Rai Moriya, Kentarou Sawano, Yusuke Hoshi, Satoru Masubuchi, Yasuhiro Shiraki, Andreas Wild, Christian Neumann, Gerhard Abstreiter, Dominique Bougeard, Takaaki Koga, and Tomoki Machida, “Cubic rashba spin-orbit interaction of a two-dimensional hole gas in a strained-Ge/SiGe quantum well,” *Phys. Rev. Lett.* **113**, 086601 (2014).
- [44] H. Nakamura, T. Koga, and T. Kimura, “Experimental evidence of cubic Rashba effect in an inversion-symmetric oxide,” *Phys. Rev. Lett.* **108**, 206601 (2012).
- [45] Matteo Michiardi, Marco Bianchi, Maciej Dendzik, Jill A. Miwa, Moritz Hoesch, Timur K. Kim, Peter Matzen, Jianli Mi, Martin Bremholm, Bo Brummerstedt Iversen, and Philip Hofmann, “Strongly anisotropic spin-orbit splitting in a two-dimensional electron gas,” *Phys. Rev. B* **91**, 035445 (2015).
- [46] K. V. Shanavas, “Theoretical study of the cubic Rashba effect at the SrTiO₃ (001) surfaces,” *Phys. Rev. B* **93**, 045108 (2016).
- [47] Hong Liu, E. Marcellina, A. R. Hamilton, and Dimitrie Culcer, “Strong spin-orbit contribution to the hall coefficient of two-dimensional hole systems,” *Phys. Rev. Lett.* **121**, 087701 (2018).
- [48] Xiong-Tao Peng, Fang Lin, Liang Chen, Lin Li, Dong-Hui Xu, and Jin-Hua Sun, “Tunable correlation effects of magnetic impurities by cubic Rashba spin-orbit coupling,” *Phys. Rev. B* **107**, 165148 (2023).
- [49] Morten Amundsen, Jacob Linder, Jason W. A. Robinson, Igor Žutić, and Niladri Banerjee, “Colloquium: Spin-orbit effects in superconducting hybrid structures,” *Rev. Mod. Phys.* **96**, 021003 (2024).
- [50] The form of the Higher order Rashba SOC terms depends on the particular symmetry directions in which the nanowire is grown [39].
- [51] Jason Alicea, “New directions in the pursuit of majorana fermions in solid state systems,” *Reports on progress in physics* **75**, 076501 (2012).
- [52] Jami J Kinnunen, Jildou E Baarsma, Jani-Petri Martikainen, and Päivi Törmä, “The Fulde-Ferrell-Larkin-Ovchinnikov state for ultracold fermions in lattice and harmonic potentials: a review,” *Reports on Progress in Physics* **81**, 046401 (2018).
- [53] Bernd Braunecker, George I. Japaridze, Jelena Klinovaja, and Daniel Loss, “Spin-selective peierls transition in interacting one-dimensional conductors with spin-orbit interaction,” *Phys. Rev. B* **82**, 045127 (2010).
- [54] Dong Liang and Xuan PA Gao, “Strong tuning of rashba spin-orbit interaction in single InAs nanowires,” *Nano Letters* **12**, 3263–3267 (2012).
- [55] Aurelien Manchon, Hyun Cheol Koo, Junsaku Nitta, Sergey M Frolov, and Rembert A Duine, “New perspectives for Rashba spin-orbit coupling,” *Nature materials* **14**, 871–882 (2015).
- [56] Dario Bercioux and Procolo Lucignano, “Quantum transport in Rashba spin-orbit materials: a review,” *Reports on Progress in Physics* **78**, 106001 (2015).
- [57] Andrew C. Potter and Patrick A. Lee, “Multichannel generalization of kitaev’s majorana end states and a practical route to realize them in thin films,” *Phys. Rev. Lett.* **105**, 227003 (2010).
- [58] Roman M. Lutchyn, Tudor D. Stanescu, and S. Das Sarma, “Search for majorana fermions in multiband semiconducting nanowires,” *Phys. Rev. Lett.* **106**, 127001 (2011).
- [59] K. T. Law and Patrick A. Lee, “Robustness of majorana fermion induced fractional josephson effect in multichannel superconducting wires,” *Phys. Rev. B* **84**, 081304 (2011).
- [60] Zhaochen Liu, Linghao Huang, and Jing Wang, “Josephson diode effect in topological superconductor,” arXiv preprint arXiv:2311.09009 (2023).
- [61] A. G. Kutlin and A. S. Mel’nikov, “Geometry-dependent effects in majorana nanowires,” *Phys. Rev. B* **101**, 045418 (2020).
- [62] A. A. Kopasov, A. G. Kutlin, and A. S. Mel’nikov, “Geometry controlled superconducting diode and anomalous josephson effect triggered by the topological phase transition in curved proximitized nanowires,” *Phys. Rev. B* **103**, 144520 (2021).
- [63] Henry F. Legg, Katharina Laubscher, Daniel Loss, and Jelena Klinovaja, “Parity-protected superconducting diode effect in topological josephson junctions,” *Phys. Rev. B* **108**, 214520 (2023).
- [64] Konstantin N. Nesterov, Manuel Houzet, and Julia S. Meyer, “Anomalous josephson effect in semiconducting nanowires as a signature of the topologically nontrivial phase,” *Phys. Rev. B* **93**, 174502 (2016).
- [65] Christian Spånslätt, “Geometric josephson effects in chiral topological nanowires,” *Phys. Rev. B* **98**, 054508 (2018).
- [66] Giovanni Vignale and I. V. Tokatly, “Theory of the nonlinear Rashba-Edelstein effect: The clean electron gas limit,” *Phys. Rev. B* **93**, 035310 (2016).
- [67] D. S. Smirnov and L. E. Golub, “Electrical spin orientation, spin-galvanic, and spin-hall effects in disordered two-dimensional systems,” *Phys. Rev. Lett.* **118**, 116801 (2017).
- [68] Erik Piatti, “Ionic gating in metallic superconductors: A brief review,” *Nano Express* **2**, 024003 (2021).